

Black-hole binary evolutions with the LEAN code

Ulrich Sperhake

Theoretisch-Physikalisches Institut, Universität Jena, Max-Wien-Platz 1, 07743 Jena,
Germany

E-mail: Ulrich.Sperhake@uni-jena.de

Abstract. Numerical simulations of black-hole binaries, obtained with the LEAN code, are presented. The code is demonstrated to produce state-of-the-art evolutions of inspiralling and merging black holes with convergent waveforms. We further compare results from head-on collisions of Brill-Lindquist and Kerr-Schild data to study the dependency of the waveforms on the choice of initial data type. In this comparison we find good qualitative agreement between the results of both data types, but observe a systematic discrepancy of about 10% in the wave amplitudes. Several attempts to explain the observed discrepancy are discussed.

1. Introduction

The era of gravitational wave physics has recently entered a very exciting stage. On the experimental side, groundbased laser interferometric detectors, GEO600, LIGO, TAMA and VIRGO, have started collecting data at or even beyond design sensitivity. Simultaneously, the modelling of the strongest source of gravitational waves, the inspiral and coalescence of black-hole binaries, has seen ground-breaking progress. Because of the complexity of the Einstein equations, the study of such systems in the framework of full general relativity is possible only by using super computers to generate numerical solutions. The extraction of physical information from such simulations is not only of fundamental importance for the detection and eventual interpretation of the observed gravitational wave patterns, but also provides valuable insight into the dynamics of compact objects and its implications for scenarios of astrophysical investigation.

The first attempts at numerically modelling black-hole-binary spacetimes dates back to the pioneering work of Eppley, Smarr and coworkers in the 1970s (see e.g. [1, 2]). Right from the start, however, numerical simulations of black-hole spacetimes were troubled by instabilities which severely inhibited progress in the ensuing decades in spite of the increasing computational resources. It is only in very recent years, that an improved insight into the formulation of the Einstein equations [3, 4, 5, 6] and coordinate or “gauge” conditions (see e.g. [7, 8, 9, 10, 11]) in combination with advanced treatment of the black hole singularities has lead to stable simulations on orbital time scales.

The first complete orbit of a black hole binary has been obtained by Brüggmann et. al. [8] by evolving black hole data of puncture type [12] using the Baumgarte-Shapiro-Shibata-Nakamura (BSSN) formulation [3, 4] in co-rotating coordinates. The first inspiral and merger of a black hole binary together with the resulting gravitational waveforms was presented by Pretorius [13] who implemented a generalized version of the harmonic formulation of the Einstein equations in the framework of special numerical techniques such as spatial compactification and implicit finite

differencing. The most recent development, now commonly referred to as “moving punctures” has been simultaneously discovered by Campanelli et. al. and Baker et. al. [14, 15, 10, 11]. Their simulations also start from puncture initial data, but allow for the punctures to move across the computational domain. Probably, the most remarkable feature of this type of simulations is that their success has now been confirmed by various groups [16, 17] and appears to generalize straightforwardly to the inclusion of spinning holes and unequal mass-ratios [18, 19, 20]. While most of the numerical work on black hole evolutions has been performed in the framework of finite differencing, spectral methods are being investigated by Scheel et. al. [21] who are able to evolve black hole orbits at relatively large separations with high accuracy.

Notwithstanding the dramatic progress in black hole simulations, there remain various open questions. With regard to the ongoing effort to detect gravitational waves, these concern in particular the accuracy and efficiency of the numerical codes. Among the primary targets of numerical relativity will be the generation of template banks of gravitational waveforms covering the parameter space of binary-black hole configurations. In view of the high dimensionality of this parameter space, especially when allowing for spinning holes, this requires a very large number of numerical simulations. Furthermore, the use of numerically generated waveforms in the process of data analysis requires high accuracy and knowledge of the remaining errors.

Inaccuracies do not only arise out of the numerical implementation, such as discretization of the equations, but are likely to also contain systematic errors, in particular related to the initial data. The difficulties in this regard are two-fold. First, initial parameters, such as the orbital angular momentum need to be chosen so as to resemble as closely as possible astrophysically realistic scenarios. Second, the construction of initial data is commonly based on single black holes described in particular types of coordinates, such as isotropic or Kerr-Schild coordinates. In the case of single black holes, the corresponding spacetime metrics are related by coordinate transformations and are known to represent physically identical configurations. Unfortunately, it is currently unknown, to what extent such uniqueness theorems generalize two binary data. In other words, given two initial data sets of a black-hole binary, to what extent can we expect these to represent the same physical configuration and thus to result in similar waveforms? In many cases, such data sets are already known to contain certain amounts of gravitational waves besides the black holes and thus do not represent identical setups.

It is a key motivation of this work to study the implications of such differences in different types of binary initial data on the resulting gravitational waveforms. For this purpose a numerical code has been developed which facilitates evolutions of black-hole binaries using different types of initial data as well as different evolution techniques. Specifically, we investigate in detail the head-on collisions of equal-mass binaries obtained from two types of initial data which have been popular in recent studies in the literature: Brill-Lindquist [22] and superposed Kerr-Schild data [23, 24].

This article is organized as follows. After describing the code in Sec. 2, we present state-of-the-art simulations of orbiting and merging black hole binaries with convergent waveforms in Sec. 3. Finally we investigate the dependency of the waveforms in the case of head-on collisions starting from a wide range of initial separations in Sec. 4 and discuss our observations.

2. The LEAN code

The LEAN code has partly been inspired by the MAYA code [25, 26, 27] and partly by the recent development of the moving puncture technique [14, 15]. A detailed description of the LEAN code has been given in [17] and we refer the reader to this work for all those aspects of the code which we only mention briefly here.

The code is based on the CACTUS computational toolkit [28] which provides parallelization, data I/O, the apparent horizon finder AHFINDERDIRECT [29, 30] and the initial data thorn TWOPUNCTURES [31]. Mesh refinement is implemented using the CARPET package [32, 33].

Dynamic mesh refinement is implemented inside the LEAN code by steering in accordance with the motion of the black holes the regriding option inherent to CARPET.

We have already mentioned the importance of the choice of formulation of the Einstein equations for achieving long-term stable evolutions. For all simulations presented in this work, we use the BSSN formulation which describes the spacetime in terms of a conformal metric $\tilde{\gamma}_{ij}$, the conformal factor e^ϕ , a conformally rescaled traceless extrinsic curvature \tilde{A}_{ij} , the trace of the extrinsic curvature K and an auxiliary connection function $\tilde{\Gamma}^i$. These variables are related to the traditional ADM variables (see, e. g. [34]) according to

$$\begin{aligned}\phi &= \frac{1}{12} \ln \gamma, & \tilde{\gamma}_{ij} &= e^{-4\phi} \gamma_{ij}, \\ K &= \gamma^{ij} K_{ij}, & \tilde{A}_{ij} &= e^{-4\phi} \left(K_{ij} - \frac{1}{3} \gamma_{ij} K \right), \\ \tilde{\Gamma}^i &= \tilde{\gamma}^{mn} \tilde{\Gamma}_{mn}^i,\end{aligned}\tag{1}$$

where γ_{ij} and K_{ij} denote the three-metric and extrinsic curvature, respectively. In addition to the Hamiltonian and momentum constraints inherent to the Einstein equations, this choice of variables leads to three auxiliary constraints, namely the definition of $\tilde{\Gamma}^i$ as well as

$$\tilde{\gamma} = \det \tilde{\gamma}_{ij} = 0 \quad \tilde{A}^i_i = 0\tag{2}$$

The exact form of the BSSN equations as used in the LEAN code, including the enforcement of constraints, is given by Eqs. (2)-(7) in [17].

In order to start the time integration, we need to prescribe initial data for all variables. In general relativity, this task is complicated by the requirement that these data solve the Einstein constraint equations, at least with good approximation. Furthermore, they need to represent an astrophysically realistic configuration. The construction of initial data thus represents a special branch of numerical relativity and we refer the reader to [35] for an overview. A key purpose of the present study is to compare the impact of the choice of initial-data on the physical results. To this end, the LEAN code facilitates evolutions of puncture or Brill-Lindquist data and superposed Kerr-Schild data.

Puncture data represent a generalization of the conformally flat Schwarzschild solution in isotropic coordinates. Brill-Lindquist data are given by the superposition of these single black hole metrics, which is obtained by merely adding the quotients in the conformal factor: $e^\phi = \sum \frac{m_i}{2|\bar{r} - \bar{r}_i|}$. Non-zero spin and momenta of the individual holes can be incorporated in the form of a non-vanishing extrinsic curvature [36]. Finally, Brandt and Brügmann cast this data into a form substantially more convenient for their use in numerical simulations and demonstrate existence and uniqueness of the solution of the Hamiltonian constraint. These data are commonly referred to as punctures and have been widely used in numerical simulations (see e. g. [7, 8, 37]).

An alternative construction of black-hole binary data which does not assume conformal flatness, is based on the single black hole solution of Kerr and Schild [23]. The superposition of two Kerr-Schild holes has been suggested in [24] and is sometimes referred to as ‘‘HuMaSh’’ data. In contrast to the Brill-Lindquist case, this superposition does not exactly satisfy the Einstein constraints even for zero spin and momenta. The constraint violations have been found to be rather small in practice, however, [38, 27] and can be made arbitrarily small by increasing the initial separation of the black holes. To our knowledge, all time evolutions of Kerr-Schild data presented in the literature have thus been obtained from this direct superposition without applying an additional constraint solving procedure (see e. g. [39, 27]).

Inside the LEAN code, ‘‘HuMaSh’’ data are obtained by superposing two Kerr-Schild holes at positions $^A x^i$ and $^B x^i$ according to

$$\gamma_{ij} = {}^A \gamma_{ij} + {}^B \gamma_{ij} - \delta_{ij},\tag{3}$$

$$K^i_j = {}^A K^i_j + {}^B K^i_j, \quad (4)$$

$$\beta_i = {}^A \beta_i + {}^B \beta_i, \quad (5)$$

$$\alpha = \left({}^A \alpha^{-2} + {}^B \alpha^{-2} - 1 \right)^{-1/2}, \quad (6)$$

Where the quantities associated with the individual holes are calculated according to Eqs. (4)–(7) in Ref. [40]. We note that with this specific superposition, lapse α and shift β^i obey the close-limit condition, i. e. they lead to the lapse and shift of a single Kerr-Schild hole in the limit of zero separation.

In addition to the evolution of the physical variables, we also need to specify conditions for the lapse function α and the shift vector β^i which incorporate the choice of coordinates or gauge. In the case of puncture and Brill-Lindquist data, we initialize lapse and shift by their flat spacetime values $\alpha = 1$, $\beta^i = 0$ and subsequently evolve these variables according to

$$\partial_t \alpha = \beta^i \partial_i \alpha - 2\alpha K, \quad (7)$$

$$\partial_t \beta^i = B^i, \quad (8)$$

$$\partial_t B^i = \partial_t \tilde{\Gamma}^i - \eta B^i. \quad (9)$$

For all simulations presented in this work, the parameter in Eq. (9) has been set to $\eta = 1$. We have also experimented with these evolution equations in the case of Kerr-Schild data, but not managed to obtain long-term stable evolutions so far. We therefore proceed differently in the Kerr-Schild evolutions and prescribe the gauge analytically along the lines of Ref. [27]. That is, we prescribe analytic trajectories ${}^A x^i(t)$, ${}^B x^i(t)$ for black holes A and B and calculate the resulting gauge functions by superposing the analytic gauge of the individual holes. Specifically, we construct polynomial functions of the type $x = y = 0$ and

$$\pm z(t) = z_0 + v_0 t + \frac{1}{2} a_0 t^2 + \frac{1}{6} j_0 t^3, \quad (10)$$

during the early stages and match these curves smoothly up to third derivatives to the constant $z = 0$ in a specified range $t_1 < t < t_2$. The exact parameters are listed in Table 1 as used for each Kerr-Schild model. Following [26] we prescribe the analytic slicing condition in the form of the densitized lapse Q . We thus obtain the superposed gauge functions

$$\beta^i = \gamma^{ij} (\beta_j^A + \beta_j^B), \quad (11)$$

$$Q = \gamma^{-1/2} \left(\alpha_A^{-2} + \alpha_B^{-2} - 1 \right)^{-1/2}. \quad (12)$$

Here the quantities denoted with an A or B are the analytic expressions for the individual black holes and γ_{ij} is the superposed metric defined in Eq. (3).

All evolution equations are implemented using the method of lines with a second order in time iterated Crank-Nicholson scheme. For the spatial discretization we use fourth order stencils for evolving punctures and second order stencils for the Kerr-Schild evolutions. The use of second order stencils in the latter case is a consequence of the use of black hole excision and the difficulties of using the wider fourth order stencils near the excision boundary (see [17] for details).

3. Orbiting black-hole binaries

Before we compare the head-on collisions of Kerr-Schild and puncture data, we demonstrate the code's capability to produce evolutions of orbiting black-hole binaries with convergent waveforms. For this purpose we consider the model *R1* of Table I of Ref. [11]. Here two black

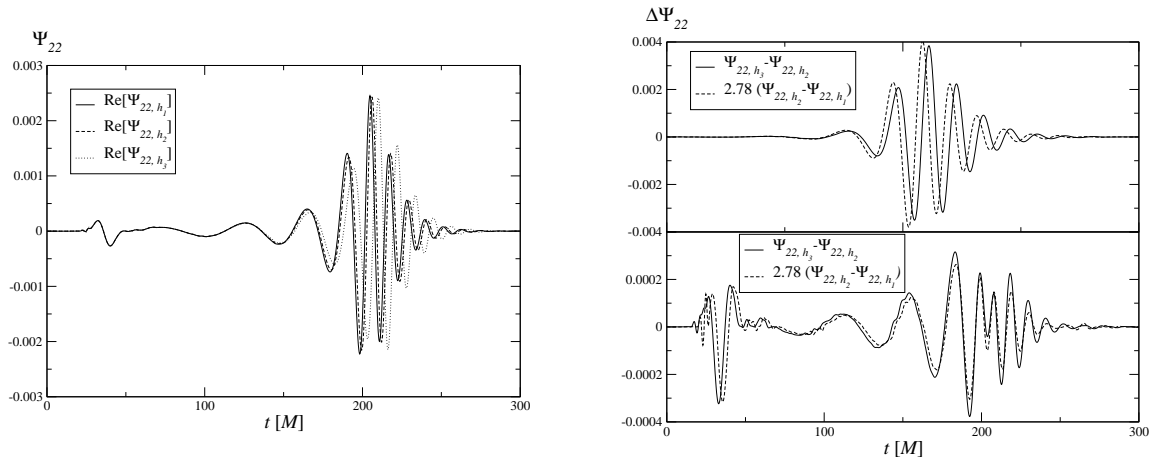


Figure 1. The $\ell = 2$, $m = 2$ waveform extracted from the *R1* simulation at $r_{\text{ex}} = 30 M$ obtained for resolutions h_1 , h_2 and h_3 (left) and convergence analysis of these results (right panel).

holes with mass parameter $m = 0.483$ start at coordinate positions $x = \pm 3.257 M$ with linear momentum parameter $P = \pm 0.133$ in the y -direction. We have evolved this configuration using eight nested refinement levels. In the coarse resolution run, we use $N_3 = 72$ points and a grid spacing of $h_3 = 5.2$ in the outermost level and double the resolution consecutively on each of the seven finer levels. The number of points is 72 for the six outer levels, while the two finest levels use 54 points each in two components centered around either hole. The corresponding setup for the medium and high resolution simulations uses finer resolutions $h_2 = \frac{4}{5}h_3$, $h_1 = \frac{3}{5}h_3$ and correspondingly larger numbers of points N_2 , N_1 .

In Fig. 1, we show the resulting Newman-Penrose scalar Ψ_4 extracted at $r = 30$ for all three simulations. We note that the waveform shows good agreement with the results obtained from similar evolutions in the literature [19, 18]. A factor two discrepancy with Fig. 2 of [18] results from a trivial rescaling depending on the choice of the eigenmode basis [cf. their Eq. (4)].

With regard to a convergence analysis, we first note that the error is dominated by the shift in phase because of the oscillating behaviour of the waveforms. We therefore study the convergence both with and without applying a phase shift to align the global maxima of the curves. These are shown in the right panel of Fig. 1 where we have amplified the differences between the higher resolution runs by a factor 2.78 expected for fourth-order convergence. The analysis shows good agreement with fourth-order convergence in both cases. These findings are in accordance with the results of [18] who also observe fourth order convergence in spite of the presence of second order ingredients in the numerical implementation.

We finally calculate the total energy radiated by the system according to Eq. (22) in Ref. [41]. At extraction radii $r = 30$ and 40 , we measure the radiated energy to be 3.48 % and 3.46 %, respectively, of the total ADM mass of the system.

4. Head-on Collisions

In this section we address the question to what extent gravitational waveforms of black-hole binary collisions depend on the type of initial data and the evolution techniques. First steps in this direction have been undertaken in the literature with regard to the initial separation of the black holes and some technical aspects of the evolution. In Ref. [42] head-on collisions of Brill-Lindquist data obtained with and without black-hole excision have been found to yield good agreement. A comparison between plunge waveforms obtained from moving puncture evolutions with those resulting from Lazarus calculations [43] has been presented in Ref. [11].

Finally, the waveforms resulting from inspiralling black holes of puncture type starting from different separations have been found to show excellent agreement in Refs. [19, 18]. To our knowledge, however, there exist no comparisons of three-dimensional simulations of black-hole binaries using conceptually different types of initial data.

In order to quantitatively address these questions, we compare the simplest type of binary simulations, namely head-on collisions of equal-mass black holes starting from rest. In this context, we note that the total amount of radiated energy is almost two orders of magnitude weaker than that obtained from orbiting binaries. Head-on collisions thus represent a particularly sensitive type of simulation for this type of analysis. In this study, we compare evolutions of Brill-Lindquist data with those of superposed Kerr-Schild data. In case of either data type, a specific initial configuration is obtained by fixing three parameters: the bare mass m of either hole, the coordinate separation D and the initial linear momenta $P_{1,2}$ of the holes. In the case of Brill-Lindquist data, the latter corresponds to the linear ADM momentum associated with the hole and we obtain a time symmetric initial data set of two holes at rest by setting $P_1 = P_2 = 0$. In the case of the Kerr-Schild data, the linear momentum of an isolated hole is given by the boost velocity parameter v . Black holes at rest are thus given by $v = 0$. Unlike the Brill-Lindquist data, however, superposed Kerr-Schild data are not time symmetric in the limit of vanishing boost parameters. The implications of non-vanishing initial velocities on the resulting gravitational waveforms will be discussed in more detail below.

In order to fix the remaining parameters m and D for both data types, we impose the conditions that the ADM mass of the total system equal unity and the irreducible masses $M_{1,2}$ are identical for both data sets. Both, for Brill-Lindquist and superposed Kerr-Schild data, the ADM mass is given by $M_{\text{ADM}} = m_1 + m_2 = 2m$ so that we set $m = 0.5$ in all simulations discussed in this section. The irreducible masses are calculated from the apparent horizon area and depend on the coordinate separation of the holes. We have thus calculated four initial data configurations with parameters listed in Table 1.

The convergence properties of both types of evolutions has been discussed in detail in Ref. [17]. There, second order convergence has been demonstrated in both cases and the errors in the waveforms arising out of the discretization have been found to be of the order of a few per cent. We now use these findings for a quantitative comparison of the gravitational waves generated by head-on collisions of Brill-Lindquist and Kerr-Schild data. The resulting real part of the $\ell = 2$, $m = 0$ mode of Ψ_4 obtained for models 1-4 of both data types are shown in Fig. 2. We first note a strong wave pulse in the Kerr-Schild evolutions starting around $t = 50$. From the timing of the pulse and its notable decrease in amplitude at larger initial separations of the holes, we interpret this feature as spurious radiation inherent to the initial data. Similar features are

Table 1. Parameters for the Brill-Lindquist and Kerr-Schild version of models 1-4. We also list the coefficients used for the gauge trajectories in the Kerr-Schild evolutions and the total radiated energy in percent of the ADM mass for both data types.

Model	D_{KS}	D_{BL}	M_{irr}	z_0	v_0	a_0	j_0	t_1	t_2	E_{KS}	E_{BL}
1	10	8.6	0.514	5	0	-0.037	0.0038	10	35	0.066	0.051
			0.514	5	-0.08	-0.0061	-0.0002	20	40	0.066	0.051
2	12	10.2	0.512	6	0	-0.029	0.0029	10	55	0.067	0.052
3	14	12.5	0.510	7	0	-0.022	0.0021	12	60	0.073	0.054
4	16	14.6	0.508	8	0	-0.021	0.0022	9.3	76	0.086	0.054

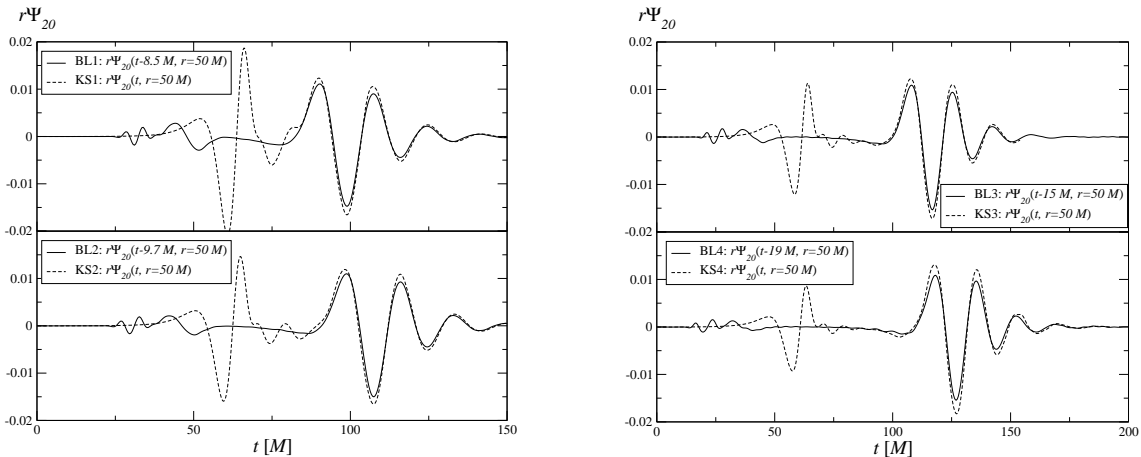


Figure 2. Real part of the $\ell = 2$, $m = 0$ mode of $r\Psi_4$ extracted at $r_{\text{ex}} = 50$ for the Kerr-Schild and Brill-Lindquist versions of model 1-4. For presentation purposes, the waveforms have been shifted in time, so that their global maximum align.

also present in the Brill-Lindquist waveforms, although with a substantially smaller amplitude.

Starting at correspondingly later times, between $t = 80$ for models 1 and $t = 120$ for model 4, the figure shows the actual wave signal generated by the head-on collisions. While the waveforms of the two data types show good qualitative agreement, we note a systematically larger wave amplitude in the case of the Kerr-Schild data by about 10 – 20 %. This discrepancy is relatively large compared with the differences encountered when evolving either data type with different grid-resolutions. Furthermore, the discrepancy does not appear to diminish as we increase the initial separation of the holes. In contrast, we observe the largest difference in the case of model 4. These results are confirmed by the calculation of the total radiated energy which is obtained from Ψ_4 by the relation

$$\frac{dE}{dt} = \lim_{r \rightarrow \infty} \left[\frac{r^2}{16\pi} \int_{\Omega} \left| \int_{-\infty}^t \Psi_4 \tilde{dt} \right|^2 d\Omega \right]. \quad (13)$$

The resulting values of E as a percentage of the total ADM energy of the system are listed in Table 1. In the calculation of these values, we have excluded the early part of the waveforms containing the spurious signal inherent to the initial data.

We next discuss several possible sources of systematic error which may be responsible for the observed discrepancies. First, we consider the possible influence of the gauge trajectories used in the evolutions of the Kerr-Schild data. While the choice of gauge does not influence the physical results in the continuum limit, at finite resolutions, gauge effects can significantly affect aspects of black-hole binary evolutions (see e.g. [37]). We therefore evolve model 1 with different gauge trajectories. We emphasize, in this context, that arbitrarily chosen trajectories will in general not result in stable simulations, and special care must be taken in specifying the parameters z_0 , v_0 , a_0 , j_0 , t_1 and t_2 . Still, there is some degree of freedom in the choice and we have listed in Table 1 two parameter sets for model 1. The corresponding trajectories are shown in the left panel of Fig. 3. The resulting waveforms plotted in the right panel of the figure are practically indistinguishable and demonstrate the robustness of the results versus the choice of gauge trajectory. In particular, this choice does not appear to account for the discrepancies observed in the head-on collisions of the Brill-Lindquist and Kerr-Schild data.

We next consider the dependency of the waveforms on the initial momenta of the black holes. We have already mentioned that Brill-Lindquist data are inherently time symmetric, whereas a

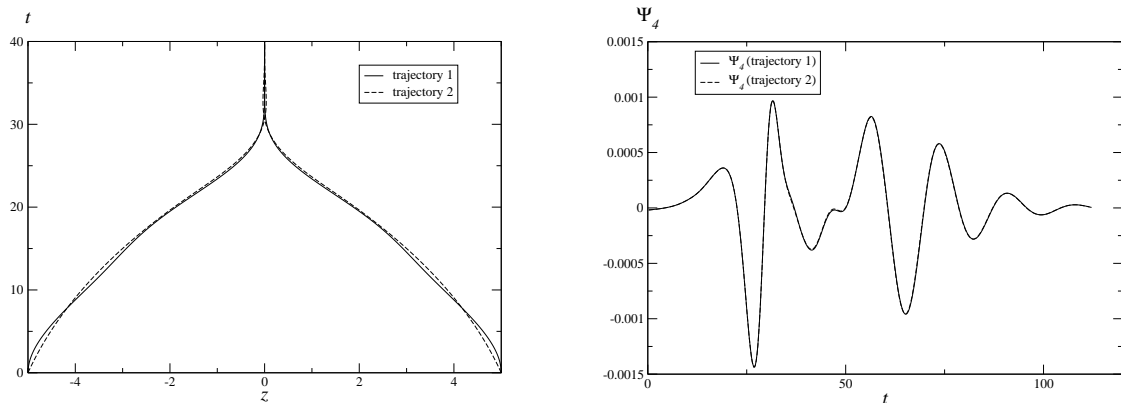


Figure 3. The two trajectories listed in Table 1 for model 2 (left panel). The resulting $\ell = 2$, $m = 0$ mode of Ψ_4 is shown in the right panel.

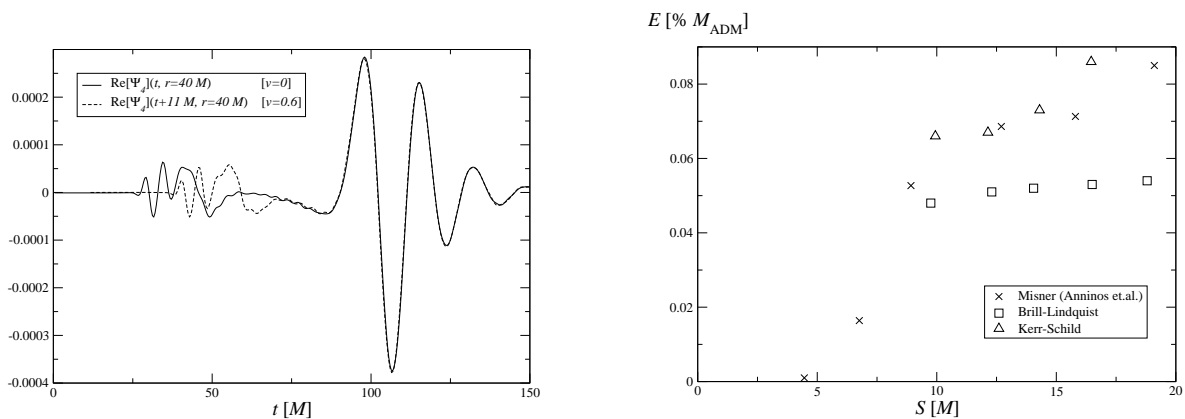


Figure 4. The $\ell = 2$, $m = 0$ mode obtained for model 2 with and without applying a non-zero linear momentum to the holes.

Figure 5. The radiated energy as a function of the initial proper-separation of the holes for Brill-Lindquist, Kerr-Schild and Misner data.

zero boost parameter does not result in time symmetry in the case of superposed Kerr-Schild data and we cannot exclude a non-vanishing initial linear momenta of the black holes. We investigate this issue by calculating the coordinate velocity of the individual Kerr-Schild holes from the central positions of the apparent horizons. In the case of model 2 we thus measure a velocity of $v = 0.06$ for either hole in the direction towards the other. We assess the impact of such a linear momentum by initializing the punctures of model 2 with a linear momentum giving rise to the same velocity. The resulting waveforms are compared in Fig. 4 and only differ by the expected shift in time. The difference in amplitude, on the other hand, is much smaller than the discrepancy between the two data types. It thus appears, that a possible difference in initial momenta of the black holes between Brill-Lindquist and Kerr-Schild data is not sufficient to account for the observed differences in amplitude.

Finally, we compare our results with those reported in [44] for head-on collisions of Misner data. For this purpose, we plot in Fig. 5 their values for the radiated energy obtained at $r_{\text{ex}} = 70$ using the Zerilli formalism as well as our results as functions of the initial three-dimensional

proper distance of the holes. The scattering of the values reported in [44] indicates fairly large error-bars, so that caution is advised in a detailed comparison. Still, we note good agreement between their results and our values for Kerr-Schild data.

It will be interesting, to recalculate the results for the Misner data using modern techniques and thus obtain more accurate values for the energy. This will facilitate a more detailed comparison with the Kerr-Schild and Brill-Lindquist data. A further interesting question is the impact of the constraint violations inherent to the superposed Kerr-Schild data. Such a study, however, represents a highly non-trivial task and requires numerical solving of a coupled set of non-linear elliptic equations in three spatial dimensions using mesh-refinement. Due to the complexity of this task, evolutions of such data have not yet been reported in the literature and are beyond the scope of this work.

Acknowledgments

I thank Markus Ansorg, Erik Schnetter and Jonathan Thornburg for providing The TWO-PUNCTURE thorn, CARPET and AHFINDERDIRECT. I further thank Bernd Brügmann, Jose Gonzalez, Mark Hannam, Sascha Husa and Christian Königsdörffer for illuminating discussions in all areas of this work. I also thank Bernard Kelly, Pablo Laguna, Ken Smith, Deirdre Shoemaker and Carlos Sopena for fruitful discussions concerning all aspects of the Kerr-Schild evolutions. This work was supported by the DFG grant SFB/Transregio 7 “Gravitational Wave Astronomy”, and computer time allocations at HLRS Stuttgart and LRZ Munich.

References

- [1] Smarr L, Čadež A, DeWitt B and Eppley K 1976 *Phys. Rev. D* **14**, 2443–2452.
- [2] Smarr L 1977 *Ann. N Y Acad. Sciences* **302**, 569–604 in Eighth Texas Symposium on Relativistic Astrophysics, ed. Papagiannis, M
- [3] Baumgarte T W and Shapiro S L 1999 *Phys. Rev. D* **59**, 024007 (*Preprint* gr-qc/9810065)
- [4] Shibata M and Nakamura T 1995 *Phys. Rev. D* **52**, 5428–5444
- [5] Bruhat Y 1962 In L Witten, (ed.), *Gravitation: An Introduction to Current Research*, : Wiley, New York.
- [6] Garfinkle D 2002 *Phys. Rev. D* **65** 044029 (*Preprint* gr-qc/0110013)
- [7] Alcubierre M, Brügmann B, Diener P, Koppitz M, Pollney D, Seidel E and Takahashi R 2003 *Phys. Rev. D* **67** 084023 (*Preprint* gr-qc/0206072)
- [8] Brügmann B, Tichy W and Jansen N 2004 *Phys. Rev. Lett.* **92** 211101 (*Preprint* gr-qc/0312112)
- [9] Pretorius F 2005 *Phys. Rev. Lett.* **95** 121101 (*Preprint* gr-qc/0507014)
- [10] Campanelli M, Lousto C O and Zlochower Y (2006) *Phys. Rev. D* **73**, 061501(R) (*Preprint* gr-qc/0601091)
- [11] Baker J G, Centrella J, Choi D-I, Koppitz M and vanMeter J 2006 *Phys. Rev. D* **73** 104002 (*Preprint* gr-qc/0602026)
- [12] Brandt S and Brügmann B 1997 *Phys. Rev. Lett.* **78** 3606–3609
- [13] Pretorius F 2005 *Class. Quantum Grav.* **22** 425–451 (*Preprint* gr-qc/0407110)
- [14] Campanelli M, Lousto C O, Marronetti P and Zlochower Y 2006 *Phys. Rev. Lett.* **96** 111101 (*Preprint* gr-qc/0511048)
- [15] Baker J G, Centrella J, Choi D-I, Koppitz M and vanMeter J 2006 *Phys. Rev. Lett.* **96** 111102 (*Preprint* gr-qc/0511103)
- [16] Herrmann F, Shoemaker D and Laguna P 2006 *Preprint* gr-qc/0601026
- [17] Sperhake U 2006 *Preprint* gr-qc/0606079.
- [18] Baker J G, Centrella J, Choi D-I, Koppitz M, vanMeter J and Miller M C 2006 *Preprint* gr-qc/0603204.
- [19] Campanelli M, Lousto C O and Zlochower Y 2006 *Phys. Rev. D* **74** 041501 (*Preprint* gr-qc/0604012)
- [20] Campanelli M, Lousto C O and Zlochower Y 2006 *Phys. Rev. D* **74** 084023 (*Preprint* gr-qc/0608275)
- [21] Scheel M A, Pfeiffer H P, Lindblom L, Kidder L E, Rinne O and Teukolsky S A 2006 *Preprint* gr-qc/0607056
- [22] Brill D R and Lindquist R W 1963 *Phys. Rev.* **131**, 471–476
- [23] Kerr R P and Schild A 1965 *Proceedings of Symposia in Applied Mathematics* vol XVII (Providence: American Mathematical Society) pp 199–209
- [24] Matzner R A, Huq M F and Shoemaker D 1998 *Phys. Rev. D* **59** 024015 (*Preprint* gr-qc/9805023)
- [25] Shoemaker D, Smith K, Sperhake U, Laguna P, Schnetter E and Fiske D 2003 *Class. Quantum Grav.* **20** 3729–3743 (*Preprint* gr-qc/0301111)

- [26] Sperhake U, Smith K L, Kelly B, Laguna P and Shoemaker D 2004 *Phys. Rev. D* **69** 024012 (*Preprint gr-qc/0307015*)
- [27] Sperhake U, Kelly B, Laguna P, Smith K L and Schnetter E 2005 *Phys. Rev. D* **71** 124042 (*Preprint gr-qc/0503071*)
- [28] Cactus Computational Toolkit homepage
- [29] Thornburg J 1996 *Phys. Rev. D* **54** 4899–4918 (*Preprint gr-qc/9508014*)
- [30] Thornburg J 2004 *Class. Quantum Grav.* **21** 743–766 (*Preprint gr-qc/0306056*)
- [31] Ansorg, M, Brüggmann B and Tichy W 2004 *Phys. Rev. D* **70** 064011 (*Preprint gr-qc/0404056*)
- [32] Carpet Code homepage
- [33] Schnetter E, Hawley S H and Hawke I 2004 *Class. Quantum Grav.* **21** 1465–1488 (*Preprint gr-qc/0310042*)
- [34] York Jr J W 1979 *Sources of Gravitational Radiation*, ed L Smarr (Cambridge: Cambridge University Press) pp 83–126
- [35] Cook G B 2000 *Living Rev. Relativity* <http://relativity.livingreviews.org/Articles/lrr-2000-5>
- [36] Bowen J M and York Jr J W 1980 *Phys. Rev. D* **21** 2047–2056
- [37] Diener P, Herrmann F, Pollney D, Schnetter E, Seidel E, Takahashi R, Thornburg J and Ventrella J 2006 *Phys. Rev. Lett.* **96** 121101 (*Preprint gr-qc/0512108*)
- [38] Marronetti P, Huq M, Laguna P, Lehner L, Matzner R and Shoemaker D 2000 *Phys. Rev. D* **62** 024017 (*Preprint gr-qc/0001077*)
- [39] Brandt S, Correll R, Gómez R, Huq M, Laguna P, Lehner L, Maronetti P, Matzner R A, Neilsen D, Pullin J, Schnetter E, Shoemaker D and Winicour J 2000 *Phys. Rev. Lett.* **85** 5496–5499 (*Preprint gr-qc/0009047*)
- [40] Bonning E, Marronetti P, Neilsen D and Matzner R A 2003 *Phys. Rev. D* **68** 044019 (*Preprint gr-qc/0305071*)
- [41] Campanelli M and Lousto C O 1999 *Phys. Rev. D* **59** 124022 (*Preprint gr-qc/9811019*)
- [42] Alcubierre M, Brüggmann B, Diener P, Herrmann F, Pollney D, Seidel E and Takahashi R 2004 *Preprint gr-qc/0411137*
- [43] Baker J, Campanelli M, Lousto C O and Takahashi R 2002 *Phys. Rev. D* **65** 124012 (*Preprint astro-ph/0202469*)
- [44] Anninos P, Hobbil D, Seidel E, Smarr L and Suen W-M 1995 *Phys. Rev. D* **52** 2044–2058